LETTER

doi:10.1038/nature09662

Quantum storage of photonic entanglement in a crystal

Christoph Clausen[1]*, Imam Usmani[1]*, Félix Bussières[1], Nicolas Sangouard[1], Mikael Afzelius[1], Hugues de Riedmatten[1,2,3] & Nicolas Gisin[1]

Entanglement is the fundamental characteristic of quantum physics—much experimental effort is devoted to harnessing it between various physical systems. In particular, entanglement between light and material systems is interesting owing to their anticipated respective roles as 'flying' and stationary qubits in quantum information technologies (such as quantum repeaters[1–3] and quantum networks[4]). Here we report the demonstration of entanglement between a photon at a telecommunication wavelength (1,338 nm) and a single collective atomic excitation stored in a crystal. One photon from an energy–time entangled pair[5] is mapped onto the crystal and then released into a well-defined spatial mode after a predetermined storage time. The other (telecommunication wavelength) photon is sent directly through a 50-metre fibre link to an analyser. Successful storage of entanglement in the crystal is proved by a violation of the Clauser–Horne–Shimony–Holt inequality[6] by almost three standard deviations ($S = 2.64 \pm 0.23$). These results represent an important step towards quantum communication technologies based on solid-state devices. In particular, our resources pave the way for building multiplexed quantum repeaters[7] for long-distance quantum networks.

Although single atoms[8,9] and cold atomic gases[10–15] are currently some of the most advanced light–matter quantum interfaces, there is a strong motivation to control light–matter entanglement with more practical systems, such as solid-state devices[16]. Solid-state quantum memories for photons can be implemented with cryogenically cooled crystals doped with rare-earth-metal ions[17], which have impressive coherence properties at temperatures below 4 K. They have the advantage of simple implementation because rare-earth-metal-doped crystals are widely produced for solid-state lasers, and closed-cycle cryogenic coolers are commercially available. Important progress has been made over the last years in the context of light storage into solid-state memories, including long storage times[18], high efficiency[19] and storage of light at the single photon level with high coherence and negligible noise[19–23]. Yet these experiments were realized with classical bright pulses or weak coherent states of light. Although this is sufficient to characterize the performance of the memory, and even to infer the quantum characteristics of the device[19,20], it is not sufficient for the implementation of more sophisticated experiments involving entanglement, as required for most applications in quantum information science. For this purpose, it is necessary to store non-classical light, in particular individual photons that are part of an entangled state (generated, for example, through spontaneous parametric down-conversion, SPDC), similar to previous demonstrations using electromagnetically induced transparency in cold atomic gases[14,15]. In addition, for quantum communication applications, the other part of the entangled state should be a photon at telecommunication wavelength in order to minimize loss during transmission in optical fibres.

In this Letter, we report on an experiment in which a photon from an entangled pair is stored in a quantum memory based on a rare-earth-metal-doped crystal. More specifically, we show that non-classical intensity correlations between the two photons still exist after storage and retrieval. We then show, through a violation of a Bell inequality, that the storage process creates a light–matter entangled state. In addition, these results represent the first successful mapping of energy–time entangled photons onto a quantum memory.

Our experiment consists of a coherent solid-state quantum memory and a source of entangled photons. A schematic of the experiment is shown in Fig. 1. The source is based on non-degenerate SPDC in a nonlinear waveguide pumped by continuous wave light at 532 nm. This yields energy–time entangled photons with the signal photon at

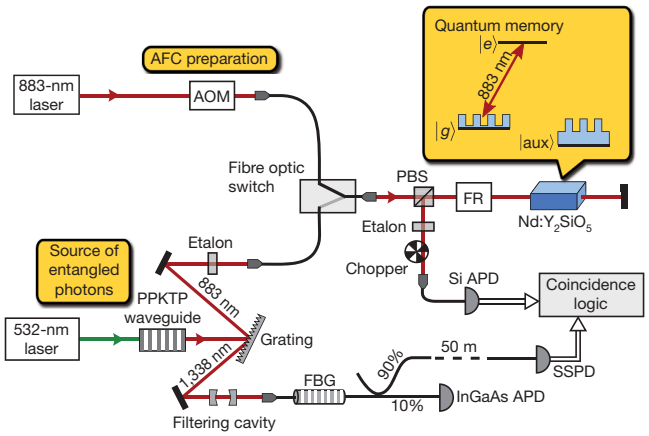

Figure 1 | Experimental set-up. The experimental set-up can be divided into three parts: the Nd:Y_2SiO_5 crystal serving as quantum memory, the laser system for the preparation of the AFC in the crystal, and the source of entangled photons with associated spectral filtering. During the experiment we periodically switch between 15 ms of AFC preparation and frequency stabilization and a 15-ms measurement phase, in which single photons are stored. During the preparation, the comb structure is prepared by frequency-selective optical pumping of atoms from the ground state $|g\rangle$ to the auxiliary state $|aux\rangle$ using light from an 883-nm diode laser in combination with an acousto-optic modulator (AOM). The fibre optic switch is in the upper position, and the silicon avalanche photodiode (Si APD) is protected from the bright light by a chopper. During the measurement phase, the positions of switch and chopper are reversed. Now, photon pairs are generated in the periodically poled potassium titanyl phosphate (PPKTP) waveguide via SPDC. The two photons in a pair are spatially separated by a diffraction grating and then strongly filtered by two etalons, a cavity and a fibre Bragg grating (FBG). Photons at 883 nm are sent through the crystal in a double-pass configuration to increase the absorption probability, and are afterwards detected by the Si avalanche photodiode. Photons at 1,338 nm are directed towards a superconducting single photon detector (SSPD) located in another laboratory 50 m away. All relevant quantities are extracted from the coincidence statistics of the two detectors. Details of the frequency stabilization and the filtering system are given in the Methods. PBS, polarizing beam splitter; FR, Faraday rotator.

[1]Group of Applied Physics, University of Geneva, CH-1211 Geneva 4, Switzerland. [2]ICFO—Institut de Ciencies Fotoniques, Mediterranean Technology Park, 08860 Castelldefels, Barcelona, Spain. [3]ICREA—Institució Catalana de Recerca i Estudis Avançats, 08015 Barcelona, Spain.
*These authors contributed equally to this work.

the memory wavelength of 883 nm, and the idler photon at the telecom wavelength of 1,338 nm. Both photons initially have a spectral width of approximately 1.5 THz, a factor of 10^4 larger than the 120-MHz bandwidth of the memory. Hence, strong filtering is crucial[14] to achieve signal-to-noise ratios sufficiently large to reveal the presence of entanglement during storage. After filtering, the signal photon is sent to the memory, and the idler photon is coupled into a fibre leading to a detector in another laboratory 50 m away. Owing to the low loss at telecommunication wavelengths, this distance could, in principle, be extended to several kilometres without significantly affecting the results presented here.

The quantum memory is a 1-cm-long Y_2SiO_5 crystal, impurity-doped with neodymium ions having a resonance at 883 nm with good coherence properties[23]. It is based on a photon-echo-type interaction using an atomic frequency comb (AFC) (see ref. 24 and Supplementary Information). In an AFC, the absorption profile of the atomic ensemble is shaped into a comb-like structure by optical pumping. A photon is then, with some efficiency, absorbed and re-emitted into a well-defined spatial mode due to a collective rephasing of the atoms in the comb structure. The time of re-emission depends on the period of the comb and is predetermined. We have previously shown that this kind of memory can store multiple temporal modes[23] and is therefore perfectly suited for storing energy–time entangled photons. For the work presented here, we have significantly improved the storage efficiency to obtain sufficiently large signal-to-noise ratios. Indeed, using a new optical pumping scheme for the preparation of the AFC (see Supplementary Information), the efficiency was increased by a factor of three for storage times below 200 ns, now reaching values up to 21% (see results below).

In a first experiment we verified that the non-classical nature of the intensity correlations between the signal (883 nm) and idler (1,338 nm) modes is preserved after the storage and retrieval process. If we assume second-order auto-correlations of signal and idler $g_x^{(2)}$ (where $x =$'s' for signal or 'i' for idler) satisfying $1 \leq g_x^{(2)} \leq 2$, then non-classicality is proved by measuring a cross-correlation $g_{si}^{(2)} = P_{si}/P_s P_i$ greater than 2 (see ref. 25). Here, P_s (or P_i) is the probability of detecting a signal (or idler) photon, and P_{si} the probability of a coincidence detection (see Methods).

We first measured $g_{si}^{(2)}$ as a function of the pump power of the source, as shown in Fig. 2a. We find an optimum around a pump power of 3 mW, where $g_{si}^{(2)} \approx 115$ without the AFC memory, and $g_{si}^{(2)} \approx 30$ after a 25-ns storage, thus proving the quantum character of the storage (note that all results presented in this Letter are without any subtraction of background noise). The reduction in the cross-correlation with the storage is due to limited efficiency (21%), which effectively increases the contribution of accidental coincidences stemming from dark counts and multiple pair emissions. Next, we measured the memory efficiency and the cross-correlation for different storage times, as shown in Fig. 2b and c.

We now turn our attention towards a particular kind of quantum correlation, namely entanglement. By performing a two-photon quantum interference experiment, we show that the entanglement of the photon pair is preserved when the signal photon is stored in the crystal.

Photon pairs generated by our source are energy–time entangled, that is, the two photons in a pair are created simultaneously to ensure energy conservation, but the pair-creation time is uncertain to within the coherence time of the pump laser. We wish to reveal the presence of this entanglement using a Franson-type set-up[5]. As detailed in the Supplementary Information, the correlations can be interpreted as stemming from local measurements performed on a post-selected time-bin entangled state: $\frac{1}{\sqrt{2}}(|E_s E_i\rangle + |L_s L_i\rangle)$, where the early and late time bins $|E_{s,i}\rangle$ and $|L_{s,i}\rangle$ are separated by a time of 25 ns set by the analysing interferometer (see Fig. 3a). In our experiment, however, the state of the signal photon is stored as a collective atomic excitation in the quantum memory before the measurement. Moreover, using a double AFC scheme[20,23], the memory is used not only to store the entangled photon, but also to analyse it as part of the measurement. More precisely, the incident time-bins $|E_s\rangle$ and $|L_s\rangle$ are mapped to distinct AFC modes $|E_{QM}\rangle$ and $|L_{QM}\rangle$, respectively (where subscript QM denotes quantum memory). Storage of the entangled signal photon then creates a light–matter entangled state:

$$\frac{1}{\sqrt{2}}(|E_{QM} E_i\rangle + |L_{QM} L_i\rangle) \quad (1)$$

The predetermined storage times of $|E_{QM}\rangle$ and $|L_{QM}\rangle$ are 75 ns and 50 ns, respectively. After absorption, both AFCs coherently re-emit the stored excitation into the same well-defined temporal and spatial mode with a relative phase $\Delta\phi_s$. This re-emission, followed by detection, constitutes the measurement of the state of the memory. The idler photon is measured using a fibre-based time-bin qubit analyser with a 25-ns delay and a relative phase $\Delta\phi_i$ between the short and long arms. The coincidence detection probability is given by:

$$P_{si} \propto 1 + V \cos(\Delta\phi_s + \Delta\phi_i) \quad (2)$$

where V is the visibility of interference. Figure 3b shows the measured coincidence rate as a function of $\Delta\phi_s$ for two values of $\Delta\phi_i$. The raw visibilities are $V = (84 \pm 4)\%$ and $(78 \pm 4)\%$.

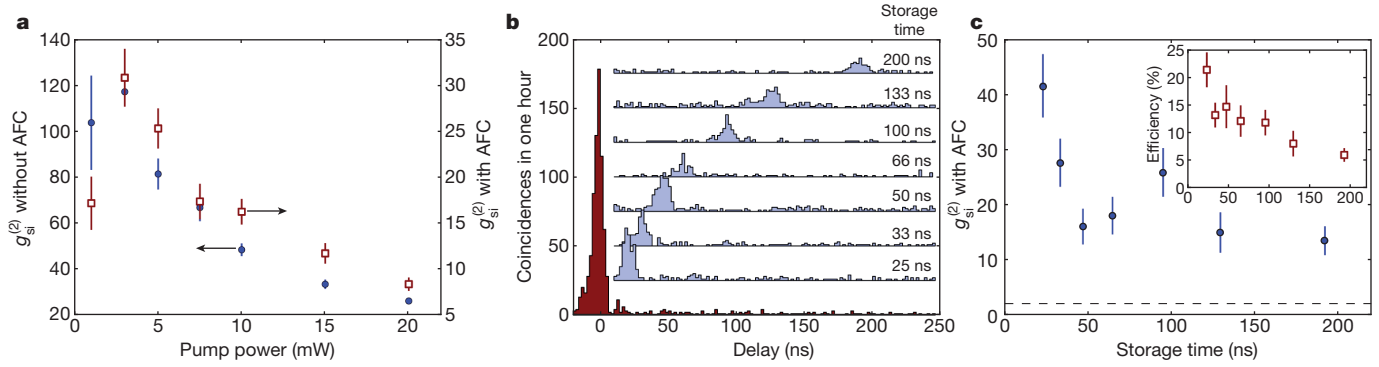

Figure 2 | Non-classical correlations and storage efficiency. **a**, Cross-correlation $g_{si}^{(2)}$ as a function of the pump power incident on the wave guide. Data points shown were taken with an AFC memory storage time of 25 ns (brown square symbols), and for comparison, with the crystal prepared with a 120-MHz-wide transmission window, that is, without AFC (blue circle symbols). The size of the coincidence window is 10 ns. **b**, Coincidence histograms for different predetermined storage times, vertically offset for clarity. For comparison, the lowest histogram was taken without AFC. The pump power was 3 mW. **c**, Cross-correlation $g_{si}^{(2)}$ as a function of storage time with 10-ns coincidence window, extracted from **b**. For storage times up to 200 ns the correlations stay well above the classical limit of $g_{si}^{(2)} = 2$ (dashed line). The inset shows the storage efficiency for the same range of storage times. With increasing storage times, limiting factors in the storage medium degrade the comb shape and reduce the efficiency and cross-correlation (see Supplementary Information). However, the latter stays well above the classical limit for storage times up to 200 ns. Error bars show ± 1 standard deviation (s.d.).

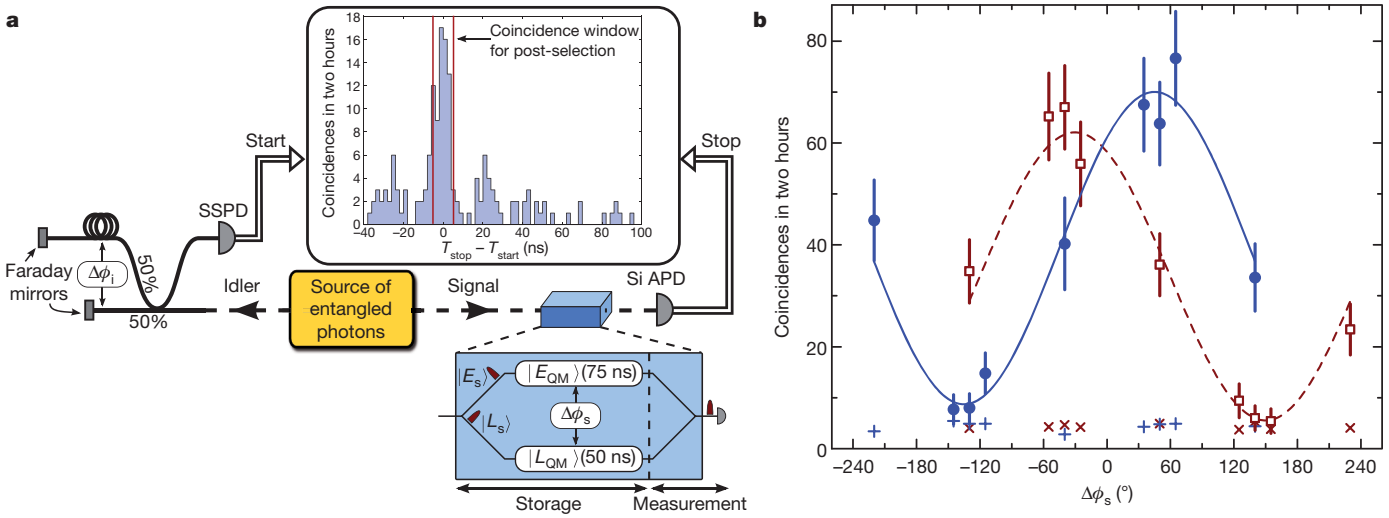

Figure 3 | Storage of photonic entanglement in a crystal. **a**, Franson-type set-up used to reveal the entanglement. A qubit analyser consisting of an unbalanced, fibre-based Michelson interferometer with 25-ns delay and relative phase $\Delta\phi_i$ is inserted before the SSPD used to detect the idler photon (see also Fig. 1). The signal photon is stored in the crystal, yielding a light–matter entangled state. The state of the memory is measured through re-emission and detection of the photon in the time-window at zero-time delay (central peak) of the coincidence histogram (inset). This post-selects measurement on the entangled state of equation (1). The relative phase $\Delta\phi_s$ can be reliably set to any desired value (see the Supplementary information). **b**, Number of coincidences in the central peak in two hours as a function of the relative phase $\Delta\phi_s$ for two values of $\Delta\phi_i$. The pump power was 5 mW, and the size of the coincidence window 10 ns. The solid and dashed lines result from fits to equation (2) and respectively give visibilities of $V = (78 \pm 4)\%$ and $(84 \pm 4)\%$. The visibilities are mainly limited by the level of accidental coincidences (cross symbols). The fit also gives a difference between the two values of $\Delta\phi_i$ of $75^\circ \pm 10^\circ$. These values closely match settings necessary for a maximal violation of the CHSH inequality. Error bars are ± 1 s.d.

Quantum entanglement can be revealed by a violation of the Clauser–Horne–Shimony–Holt (CHSH) inequality[6]. The possibility of violating this inequality, that is, of finding a CHSH parameter $S > 2$, can be inferred indirectly from a visibility larger than $1/\sqrt{2} \approx 70.7\%$. Nevertheless, we performed the measurements necessary for a direct violation of the inequality and obtained $S = 2.64 \pm 0.23$. This proves the presence of entanglement between the idler photon and the matter qubit in the crystal, provided the effect of the memory on single photons is appropriately described as storage followed by measurement (see Supplementary Information). This description is correct within the theory of AFC memories[24], which is supported by experiments storing weak coherent states of light[11,21–23]. Note also that we do not claim any demonstration of nonlocal correlations. Indeed, besides the usual locality and detection loopholes, here the measurement setting has to be chosen before the photonic qubit is mapped onto the crystal. This could have been avoided by adding an interferometer after the memory, the latter being used for storage only. We did not do so because we think that it is elegant and simple to use the memory also as a small quantum processor that performs the measurement.

A particularly intriguing situation arises when post-selecting on the case where only $|E_s\rangle$ is stored in the crystal for 25 ns using a single AFC scheme, while $|L_s\rangle$ is directly transmitted. Indeed, the imbalance between the storage efficiency and the transmission probability offers a well-suited qubit analyser for a violation of the CHSH inequality using bases lying in the x–z plane of the Bloch sphere. We performed such a measurement and observed $S = 2.62 \pm 0.15$ (see Supplementary Information). This implies that the initial photon–photon entangled state is mapped onto a state of the form:

$$\sqrt{\eta_{abs}}|E_{QM}E_i\rangle + |L_sL_i\rangle \qquad (3)$$

where η_{abs} is the absorption efficiency. This is an entangled state between a telecommunication-wavelength qubit and a light–matter hybrid qubit. We note that this kind of hybrid qubit is the key ingredient of an efficient quantum repeater protocol based on atomic ensembles and linear optics[3].

This work is part of the effort towards implementing a quantum repeater, which could provide a solution to the distance limit (due to intrinsic loss) for entanglement distribution and quantum cryptography using optical fibres[3]. To achieve this long-term goal, several future advances are required. The user must be able to trigger the re-emission of the memory, whereas in our experiment the duration of the storage is pre-determined. We have proposed[24] and demonstrated[26] a method for achieving on-demand re-emission using so-called spin-wave storage. This has the additional benefit of allowing longer storage times owing to the more robust spin coherence. Another crucial aspect is the efficiency, which is directly linked to the optical depth of the material[24]. It can be increased by using longer crystals[19] or optical cavities[27,28].

The creation of entanglement between a single photon and a macroscopic object—in this case a single collective atomic excitation delocalized over a 1-cm-long crystal—is fascinating in itself. Beyond its fundamental interest, we believe that our demonstration of storage of entanglement in a crystal represents an important step towards quantum repeaters based on solid-state quantum memories.

We note that, parallel to this work, Saglamyurek *et al.* have demonstrated storage and retrieval of an entangled photon using a thulium-doped lithium niobate waveguide[29].

METHODS SUMMARY

Spectral filtering and detection. The bandwidth of the photon pairs is reduced by a factor of 10^4 in several steps. Pump, signal and idler photons are spatially separated by a diffraction grating (see Fig. 1). In combination with coupling into single-mode fibres, this reduces the bandwidth to tens of gigahertz. A subsequent passage through a Fabry–Perot cavity reduces the bandwidth of the idler photon to 45 MHz (corresponding to a coherence time of about 4 ns), and a fibre Bragg grating blocks all but one of the longitudinal cavity modes. The signal photon is filtered by two etalons with a linewidth of 600 MHz each, and different free spectral ranges. The detector efficiency is 8% for the idler photon with 10-Hz dark counts, and 30% with 100-Hz dark counts for the signal photon.

Frequency stabilization. We must ensure, for the whole duration of a measurement, that the central frequency of the optical filtering system at 1,338 nm and of the AFC at 883 nm both satisfy the energy conservation of the SPDC process. To do this, a small fraction of the light at 883 nm is overlapped with the light of the 532-nm laser that pumps the PPKTP waveguide. This leads to the creation of light at 1,338 nm by difference frequency generation (DFG). Using this DFG signal, the frequency of the 532-nm light is adjusted such that the detection rate on a separate InGaAs avalanche photodiode (see Fig. 1) stays constant, which means that the 1,338-nm DFG light is in resonance with the filtering cavity. Long-term stability of the 883-nm laser itself is achieved by continuously referencing it to a Fabry–Perot cavity.

Full Methods and any associated references are available in the online version of the paper at www.nature.com/nature.

Received 24 August; accepted 9 November 2010.
Published online 12 January 2011.

1. Briegel, H.-J., Dür, W., Cirac, J. I. & Zoller, P. Quantum repeaters: the role of imperfect local operations in quantum communication. *Phys. Rev. Lett.* **81,** 5932–5935 (1998).
2. Duan, L.-M., Lukin, M. D., Cirac, J. I. & Zoller, P. Long-distance quantum communication with atomic ensembles and linear optics. *Nature* **414,** 413–418 (2001).
3. Sangouard, N., Simon, C., de Riedmatten, H. & Gisin, N. Quantum repeaters based on atomic ensembles and linear optics. Preprint at ⟨http://arxiv.org/abs/0906.2699⟩ (2009).
4. Kimble, H. J. The quantum internet. *Nature* **453,** 1023–1030 (2008).
5. Franson, J. D. Bell inequality for position and time. *Phys. Rev. Lett.* **62,** 2205–2208 (1989).
6. Clauser, J. F., Horne, M. A., Shimony, A. & Holt, R. A. Proposed experiment to test local hidden-variable theories. *Phys. Rev. Lett.* **23,** 880–884 (1969).
7. Simon, C. *et al.* Quantum repeaters with photon pair sources and multimode memories. *Phys. Rev. Lett.* **98,** 190503 (2007).
8. Blinov, B. B., Moehring, D., Duan, L.-M. & Monroe, C. Observation of entanglement between a single trapped ion and a single photon. *Nature* **428,** 153–157 (2004).
9. Volz, J. *et al.* Observation of entanglement of a single photon with a trapped atom. *Phys. Rev. Lett.* **96,** 030404 (2006).
10. Matsukevich, D. N. *et al.* Entanglement of a photon and a collective atomic excitation. *Phys. Rev. Lett.* **95,** 040405 (2005).
11. de Riedmatten, H. *et al.* Direct measurement of decoherence for entanglement between a photon and stored atomic excitation. *Phys. Rev. Lett.* **97,** 113603 (2006).
12. Chen, S. *et al.* Demonstration of a stable atom-photon entanglement source for quantum repeaters. *Phys. Rev. Lett.* **99,** 180505 (2007).
13. Sherson, J. F. *et al.* Quantum teleportation between light and matter. *Nature* **443,** 557–560 (2006).
14. Akiba, K., Kashiwagi, K., Arikawa, M. & Kozuma, M. Storage and retrieval of nonclassical photon pairs and conditional single photons generated by the parametric down-conversion process. *N. J. Phys.* **11,** 013049 (2009).
15. Jin, X.-M. *et al.* Quantum interface between frequency-uncorrelated down-converted entanglement and atomic-ensemble quantum memory. Preprint at ⟨http://arxiv.org/abs/1004.4691⟩ (2010).
16. Togan, E. *et al.* Quantum entanglement between an optical photon and a solid-state spin qubit. *Nature* **466,** 730–734 (2010).
17. Tittel, W. *et al.* Photon-echo quantum memory in solid state systems. *Laser Photon. Rev.* **4,** 244–267 (2010).
18. Longdell, J. J., Fraval, E., Sellars, M. J. & Manson, N. B. Stopped light with storage times greater than one second using electromagnetically induced transparency in a solid. *Phys. Rev. Lett.* **95,** 063601 (2005).
19. Hedges, M. P., Longdell, J. J., Li, Y. & Sellars, M. J. Efficient quantum memory for light. *Nature* **465,** 1052–1056 (2010).
20. de Riedmatten, H., Afzelius, M., Staudt, M. U., Simon, C. & Gisin, N. A solid-state light-matter interface at the single-photon level. *Nature* **456,** 773–777 (2008).
21. Chanelière, T., Ruggiero, J., Bonarota, M., Afzelius, M. & Gouët, J.-L. L. Efficient light storage in a crystal using an atomic frequency comb. *N. J. Phys.* **12,** 023025 (2010).
22. Sabooni, M. *et al.* Storage and recall of weak coherent optical pulses with an efficiency of 25%. *Phys. Rev. Lett.* **105,** 060501 (2010).
23. Usmani, I., Afzelius, M., de Riedmatten, H. & Gisin, N. Mapping multiple photonic qubits into and out of one solid-state atomic ensemble. *Nature Commun.* **1,** 12 (2010).
24. Afzelius, M., Simon, C., de Riedmatten, H. & Gisin, N. Multimode quantum memory based on atomic frequency combs. *Phys. Rev. A* **79,** 052329 (2009).
25. Kuzmich, A. *et al.* Generation of nonclassical photon pairs for scalable quantum communication with atomic ensembles. *Nature* **423,** 731–734 (2003).
26. Afzelius, M. *et al.* Demonstration of atomic frequency comb memory for light with spin-wave storage. *Phys. Rev. Lett.* **104,** 040503 (2010).
27. Afzelius, M. & Simon, C. Impedance-matched cavity quantum memory. *Phys. Rev. A* **82,** 022310 (2010).
28. Moiseev, S. A., Andrianov, S. N. & Gubaidullin, F. F. Efficient multimode quantum memory based on photon echo in an optimal QED cavity. *Phys. Rev. A* **82,** 022311 (2010).
29. Saglamyurek, E. *et al.* Broadband waveguide quantum memory for entangled photons. *Nature* doi:10.1038/nature09719 (this issue).

Supplementary Information is linked to the online version of the paper at www.nature.com/nature.

Acknowledgements We thank R. Locher for help during the early stages of the experiment. We are grateful to A. Beveratos and W. Tittel for lending us avalanche photodiodes. This work was supported by the Swiss NCCR Quantum Photonics, the Science and Technology Cooperation Program Switzerland–Russia, as well as by the European projects QuRep and ERC-Qore. F.B. was supported in part by FQRNT.

Author Contributions All authors contributed extensively to the work presented in this paper.

Author Information Reprints and permissions information is available at www.nature.com/reprints. The authors declare no competing financial interests. Readers are welcome to comment on the online version of this article at www.nature.com/nature. Correspondence and requests for materials should be addressed to M.A. (mikael.afzelius@unige.ch).

METHODS

Spectral filtering and detection. The narrowband filtering of the SPDC photons consists of several steps (see Fig. 1). First, a diffraction grating spatially separates the pump, signal and idler photons and, in combination with coupling into single-mode fibres, reduces the bandwidth of the photons at 883 nm (or 1,338 nm) to 90 GHz (or 60 GHz). Photons at 1,338 nm are then coupled through a Fabry–Perot cavity with linewidth 45 MHz and free spectral range of 23.9 GHz. Subsequently, a fibre Bragg grating with 16 GHz bandwidth ensures that only a single longitudinal cavity mode remains.

Filtering one of the photons in the pair is the same as filtering the photon pair as a whole, because energy conservation guarantees that photons measured in coincidence have the same bandwidth. However, uncorrelated photons would then contribute significantly to the accidental coincidences. Therefore, complementary filtering at 883 nm was necessary. To do this, we used one solid and one air-spaced etalon, both with bandwidths around 600 MHz. Different free spectral ranges of 42 and 50 GHz eliminate uncorrelated longitudinal modes. Additionally, outside the 120-MHz bandwidth of the AFC, the absorption of the crystal with an inhomogeneous linewidth of 6 GHz provides a final filtering step.

We used detectors with 30% detection efficiency and approximately 100 Hz dark counts at 883 nm, and detectors with 8% detection efficiency and approximately 10 Hz at 1,338 nm. Together with a transmission of the filtering system for the signal (or idler) photon of 45% (or 14%), and 4% (or 14%) for the remainder of the optical set-up, we reached an overall detection efficiency of 0.5% (or 0.15%) (see also Supplementary Information). These numbers could, in principle, be significantly improved through optimized optical alignment, the use of anti-reflection-coated elements, and so on.

Frequency stabilization. In the experiment, coincidence rates are typically a few per minute. With accumulation times thus reaching several hours, a high degree of frequency stability of the lasers and filtering elements is indispensable. In particular, frequency drifts of the AFC preparation laser with respect to the pump laser of the SPDC source have to be eliminated. Otherwise, the photon-pair frequencies $\omega_{883} + \omega_{1338} = \omega_{532}$ imposed by energy conservation in the SPDC would not simultaneously match the centre of the AFC and that of the filtering system at 1,338 nm. Drifts were eliminated using the following method. First, the long-term stability of the 883-nm laser was dramatically increased by locking it to a temperature-stabilized Fabry–Perot cavity. Second, during the 15-ms preparation cycle, we injected a fraction of the 883-nm light into the waveguide. The frequency of the light created at 1,338 nm via difference frequency generation (DFG) was tuned by controlling the frequency of the pump laser at 532 nm. Using a side-of-fringe technique, we could then lock the frequency of the DFG signal to the transmission peak of the filtering cavity. As a result, long-term frequency deviations between the centre of the AFC structure and the filtered photon pairs were reduced to about 1 MHz over several hours.

For measurements involving the unbalanced Michelson interferometer for the idler photon, the phase of the interferometer was also stabilized using the highly coherent DFG light.

Photon correlations in SPDC. Neglecting the exact frequency dependence, the state of the photons created in the SPDC process is described by $|0_s, 0_i\rangle + \sqrt{p}|1_s, 1_i\rangle + O(p)$, where the subscript 's' (or 'i') indicates the signal (or idler) mode at 883 nm (or 1,338 nm). Here, the pair creation probability p is assumed to be small and proportional to the pump power. In such a state, the signal and idler modes individually exhibit the statistics of a classical thermal field, that is, their auto-correlations are $g_x^{(2)} = 2$ for $x =$ s or i. We stress, however, that the criterion for non-classicality of the cross-correlation that we used, namely $g_{si}^{(2)} = P_{si}/P_s P_i > 2$, requires only that $1 \leq g_x^{(2)} \leq 2$, which is always fulfilled by non-degenerate photon pairs created through SPDC. In practice, P_{si} (or $P_s P_i$) is determined by the number of coincidences in a certain time window centred on (or away from) the coincidence peak. For low pump powers, the measured cross-correlation is usually limited by detector dark counts, and at high pump powers it is reduced by the contribution of multiple pairs, that is, higher-order terms in p.